
ENHANCING MARITIME TRAJECTORY FORECASTING VIA H3 INDEX AND CAUSAL LANGUAGE MODELLING (CLM)

Nicolas Drapier*

PRISME Laboratory, SAS Impact
University of Orléans
Orléans, France

nicolas.drapier@etu.univ-orleans.fr, nicolas.drapier@sas-impact.fr

Aladine Chetouani†

PRISME Laboratory
University of Orléans
Orléans, France

aladine.chetouani@univ-orleans.fr

Aurélien Chateigner‡

SAS Impact
Orléans, France

aurelien.chateigner@sas-impact.fr

ABSTRACT

The prediction of ship trajectories is a growing field of study in artificial intelligence. Traditional methods rely on the use of LSTM, GRU networks, and even Transformer architectures for the prediction of spatio-temporal series. This study proposes a viable alternative for predicting these trajectories using only GNSS positions. It considers this spatio-temporal problem as a natural language processing problem. The latitude/longitude coordinates of AIS messages are transformed into cell identifiers using the H3 index. Thanks to the pseudo-octal representation, it becomes easier for language models to learn the spatial hierarchy of the H3 index. The method is compared with a classical Kalman filter, widely used in the maritime domain, and introduces the Fréchet distance as the main evaluation metric. We show that it is possible to predict ship trajectories quite precisely up to 8 hours with 30 minutes of context. We demonstrate that this alternative works well enough to predict trajectories worldwide.

Keywords Maritime Trajectory Prediction · H3 Index · Causal Language Modelling (CLM) · GPS Coordinate Discretisation

1 Introduction

Predicting ship trajectories is an essential task for maritime stakeholders, encompassing economic, security, and logistical considerations. Accurate trajectory prediction plays a pivotal role in optimising shipping routes, ensuring maritime safety, and managing resources efficiently. However, this endeavour has posed several challenges due to the vast amount of trajectory data generated in real-time and the intricate interplay of spatial and temporal factors.

Traditionally, Long Short-Term Memory (LSTM) [1] and Gated Recurrent Units (GRU) [2] networks have been employed to model sequential and temporal data, and many researchers have tried to adapt these recurrent neural network (RNN) architectures to the spatio-temporal domain. While these RNN-based approaches have demonstrated success in various applications [3, 4, 5, 6], they typically neglect the crucial spatial component inherent in ship trajectories, such as the geographical coordinates and the intricate relationships between waypoints in a trajectory.

*Principal author, Conceptualisation, Methodology, Software, Validation, Formal analysis, Investigation, Resources, Data Curation, Writing – original draft, Visualisation

†Writing – review & editing, Visualisation, Supervision, Project administration

‡Conceptualisation, Methodology, Validation, Formal analysis, Writing – review & editing, Visualisation, Supervision, Project administration

More recently, the introduction of the Transformer architecture [7] by Vaswani et al. has sparked a revolution in different fields, such as the Natural Language Processing (NLP) [8, 9, 10] and time-series prediction [11, 12, 13, 14], democratising the development of state-of-the-art models due to their popularity, scalability, and ease of use. Models like Informer [15] and Autoformer [16] have shown exceptional prowess in capturing long-term dependencies and intricate relationships within temporal data, making them valuable tools in the realm of time-series prediction.

However, despite their successes in temporal modelling, these models based on the Transformer architecture have not been adequately tailored to address the spatial nuances inherent in ship trajectories, limiting their applicability in the maritime domain. This research effort seeks to bridge this gap by exploring novel approaches that combine the strengths of Transformer-based architectures with spatial awareness, offering the potential to revolutionise ship trajectory prediction in real-time industrial applications. In doing so, we aim to address the limitations of existing models, making maritime operations more efficient, secure, and economically viable.

We believe that combining Transformer-based models with better spatial representation can enhance the accuracy of ship trajectory prediction. In maritime trajectory prediction, accurately representing Global Navigation Satellite System (GNSS) coordinates is challenging due to the inherent precision of GNSS measurements. Even a minor error of one hundredth of a degree in latitude consistently translates to a difference of approximately 1.11 kilometres, while in longitude, the impact varies considerably based on Earth’s location. For instance, at the equator, it approximates 1.11 kilometres, but at 80° longitude, it diminishes to around 200 metres. These variations lead to profound disparities in actual locations, making it difficult to increase the dimensionality of GNSS positions using an autoencoder-based approach.

In light of these considerations, we set out to explore an alternative solution: the discretisation method utilising Uber’s Hexagonal Hierarchical Spatial Index (H3) index [17]. H3 is a geospatial indexing system that partitions the world into hexagonal cells. H3 cells are written to 64 bits and can be represented in hexadecimal format, providing a creative solution to the challenges associated with the continuous representation of GNSS coordinates. Our central aim with this discretisation approach is to reconfigure a ship’s trajectory from Automatic Identification System (AIS) ⁴ messages [18] into a structured narrative, akin to the composition of words in a sentence. By doing so, we effectively counteract the potential detrimental impacts of minor coordinate inaccuracies, and we expect to benefit from the ability of Transformer architectures to understand the relationships between tokens.

Given the limited usefulness of the initial 12 bits of the H3 cells for improving our understanding of space, we propose an innovative representation. Our aim here is to optimise the cell representation, driven by the need to alleviate computational overhead and establish a more streamlined tokeniser vocabulary, consisting of just 270 tokens. This tailored approach not only enhances the efficiency of processing ship trajectories but also seamlessly aligns them with Transformer-based models equipped with spatial awareness, as envisioned in this research.

In the forthcoming sections, we delve into the methodologies adopted, with a primary emphasis on the utilisation of the H3 index for spatial representation. We elaborate on the rationale behind this choice and its potential to enhance ship trajectory prediction models. Furthermore, we present experimental results and validate our approach against existing methods, demonstrating the promise of integrating Transformer architectures with spatial awareness within the maritime domain.

2 Background

GNSS play a pivotal role in modern artificial intelligence, particularly in applications related to Geospatial Intelligence (GEOINT). GEOINT, as defined by the USA, refers to the analysis and exploitation of geospatial information to gain insights and support joint operations [19, 20]. GNSS, which includes systems like GPS, GLONASS, and Galileo provides essential geospatial data that underpins these intelligence operations.

A complementary technology in the maritime domain is the Automatic Identification System (AIS) [18], which is increasingly intertwined with GNSS systems. AIS transponders on ships broadcast their GNSS-derived positions, allowing for real-time tracking and identification. This integration has revolutionised maritime operations, enabling vessel tracking, collision avoidance, and efficient port management.

However, AIS is limited due to inherent characteristics. The protocol’s reliance on VHF radio transmissions limits its range, making it susceptible to signal loss in remote or congested areas and not always accurate due to delays in transmitting the data. Additionally, while AIS data provides valuable information, it may not always reflect the full scope of a vessel’s activities, particularly in scenarios involving illicit or evasive behaviour.

⁴The *Automatic Identification System* is an automatic tracking system used to monitor and locate ships in real time. It uses Very High Frequency (VHF) transceivers to transmit data such as the vessel’s identifier, position, speed and direction.

One of the fundamental challenges in utilising GNSS and AIS data is the open nature of the ocean. Unlike terrestrial environments, where fixed road networks and landmarks facilitate navigation, the vast and unpredictable expanse of the sea makes it difficult to determine a vessel’s trajectory with absolute certainty. The dynamic and often erratic nature of maritime operations poses significant obstacles to generating accurate predictions.

In the field of natural language processing (NLP) research, Transformer architectures with progressively extended model capabilities are at the heart of research. They are originally designed for NLP applications, and they have undergone substantial improvements in order to optimise their efficiency in the processing of sequential data. Recent progress in this line of research has been directed towards improving their ability to handle extended sequences efficiently [21, 22, 23, 24, 25, 26], making transformers an appropriate choice for the complex analysis of large datasets on maritime trajectories.

3 Related Work

In recent years, the field of vessel trajectory prediction and maritime safety has witnessed significant developments, driven by advances in artificial intelligence and the utilisation of AIS data. Researchers have been actively working towards enhancing the safety and efficiency of maritime systems, particularly in the context of collision avoidance.

A comprehensive survey by Tu et al. [27] examines the exploitation of AIS data for intelligent maritime navigation. AIS, which tracks vessel movements through electronic data exchange, offers valuable insights for maritime safety, security, and efficiency. This survey explores various facets of AIS data sources and their applications, including traffic anomaly detection, route estimation, collision prediction, and path planning. It underscores the synergy between data and methodology in marine intelligence research, highlighting the importance of both components.

Although the utilisation of autoencoders in vessel trajectory prediction shows promise based on theoretical merits, some concerns can be raised about their practical application. For instance, the study presented in [28] by Murray and Prasad Perera proposes a novel dual linear autoencoder method for predicting vessel trajectories using historical AIS data and unsupervised learning for trajectory clustering and classification. This technique offers several advantages, such as generating multiple possible trajectories and estimating positional uncertainties through latent distribution estimation. However, critics argue that the method may only provide accurate predictions for short time horizons, typically less than 30 minutes, given its reliance on a single initial condition or current position in the trajectory. Additionally, since the algorithm operates based on previously observed states, it might struggle to effectively process new, unseen data. Thus, further investigation into enhancing the adaptability and accuracy of autoencoder-based approaches for longer-term vessel trajectory predictions is warranted.

To address the complexity of maritime traffic patterns and improve Maritime Situational Awareness, Pallotta et al. have introduced methodologies like Traffic Route Extraction and Anomaly Detection (TREAD) [29]. TREAD relies on unsupervised and incremental learning to extract maritime movement patterns from AIS data. It serves as the basis for automatic anomaly detection and trajectory projection, enabling more effective synthesis of relevant behaviours from raw data to support decision-making processes. Trajectory predictions are made by context-based tracking algorithms, using the direction of mean velocity and the series of trajectories taken by other vessels of the same type. However, the trajectory of a fishing vessel is highly anarchic and follows the movements of shoals of fish. It is very difficult to model such behaviour by taking account of positions alone. The statistical model used is based on automatic knowledge discovery. We believe that its ability to predict ship movements away from shipping routes is limited because the context of other ships at the same location is reduced or non-existent.

In the context of increasing concerns about collision accidents in the shipping industry, an advanced ship trajectory prediction model has been proposed [30]. This model combines a multi-head attention mechanism with bidirectional gate recurrent units (MHA-BiGRU) to enhance precision and real-time capabilities in AIS-based ship trajectory prediction. It effectively retains long-term sequence information, filters and modifies historical data, and models associations between past and future trajectory states, ultimately leading to improved accuracy. But, the approach taken in this model raises certain concerns, particularly regarding the normalisation of longitude and latitude data. While this is a common practice in trajectory prediction models, it can lead to potential inaccuracies. Normalising these coordinates to a 0-1 scale can distort critical spatial relationships, especially near meridians and poles. This simplification might also inadequately represent the real-world physical distance, as a degree’s distance varies with latitude. Such distortions are crucial in the shipping industry, where precision in trajectory prediction is paramount for collision avoidance. In 2022, the French Bureau d’enquêtes des évènements de mer (BEAMer) recorded 472 accidents, 68% of which were caused by fishing vessels [31].

Urban mobility research has also contributed to the understanding of human transportation modes. TrajectoryNet [32], a neural network architecture for point-based trajectory classification using GPS traces, offers an innovative

perspective. It embeds the original feature space into a higher-dimensional representation, enriches the feature space with segment-based information, and employs Maxout activations to enhance the predictive power of Recurrent Neural Networks (RNNs). TrajectoryNet achieves impressive classification accuracy when identifying various transportation modes from GPS traces. Significantly, we were particularly inspired by the application of NLP techniques in this context. The concept of embedding, commonly used in NLP to convert words into vector representations, resonated with us for its potential in our own research. We admired how this approach effectively captures the underlying semantics of continuous features, like speed, in varying contexts. This insight guided us in designing our experiment, where we aimed to similarly interpret and represent the semantics of continuous geospatial features, providing a richer understanding of the data beyond its numerical value.

While the use of Automatic Identification System (AIS) data for predicting vessel trajectories has seen significant advancements, such as the successful deployment of the TrAISformer model by Nguyen et al. [33], however, there are a number of areas for improvement regarding this approach. The TrAISformer model represents an innovative step forward by employing a discretised, multidimensional encoding of AIS data and introducing a distinctive loss function tailored to handle variability and multiple modes within shipping movement data. However, it is important to note that traditional spatial binning techniques [34] have proven effective for local entity analysis. Nevertheless, these methods face considerable challenges when attempting to scale up for global applications due to resource limitations. Therefore, while the TrAISformer model presents a promising solution, further research is required to assess its efficacy under diverse operational conditions and evaluate its potential impact on computational resources.

These various projects represent a selection of research activities that have made significant contributions to the advancement of ship trajectory prediction, the use of AIS data and maritime safety. This research study builds on these foundations and presents a unique approach to GNSS coordinate discretisation and trajectory prediction using transformer architectures.

4 Methodology

This section details the methodology described above. The cornerstone of our approach is the transformation of the traditional latitude/longitude coordinate system into a pseudo-octal format using the H3 index. On this basis, we deploy a simplified version of the Mixtral 8x7B model specifically adapted for trajectory prediction. The aim of this adaptation is to make the model accessible for execution on consumer computers while minimising its resource requirements. To assess the accuracy of our predictions, we introduce the use of the Fréchet distance, which serves as a robust measure for evaluating the quality of predictions. The summary is given in the figure 1.

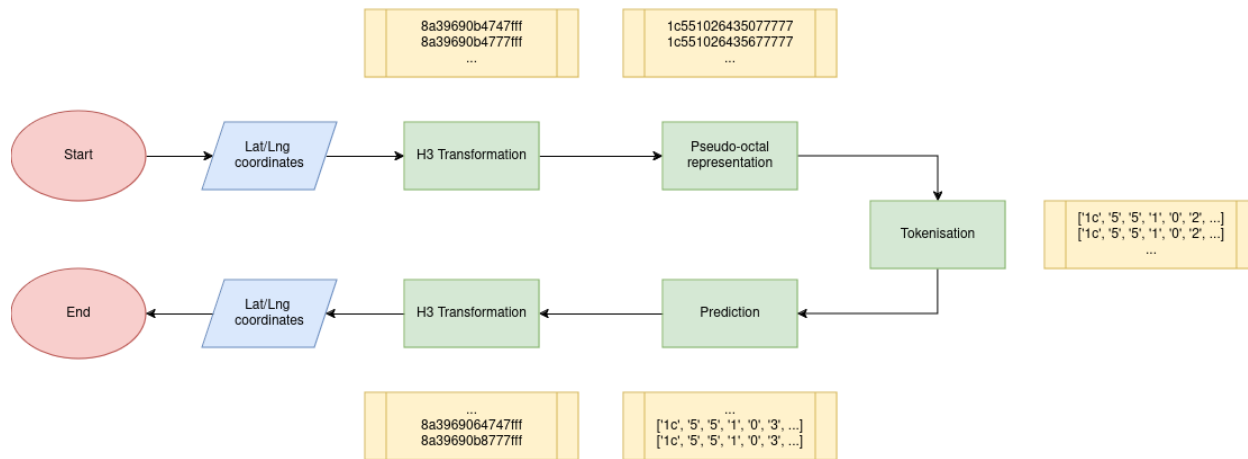


Figure 1: Flowchart of the method presented throughout the article. Green rectangles represent transformation processes, yellow rectangles correspond to examples.

4.1 H3 Index

The methodology section of this research paper delves into crucial decisions that form the basis of our innovative approach in maritime trajectory prediction. In this section, we explore the pivotal choice of utilising the H3 index developed by Uber as the cornerstone of our spatial representation.

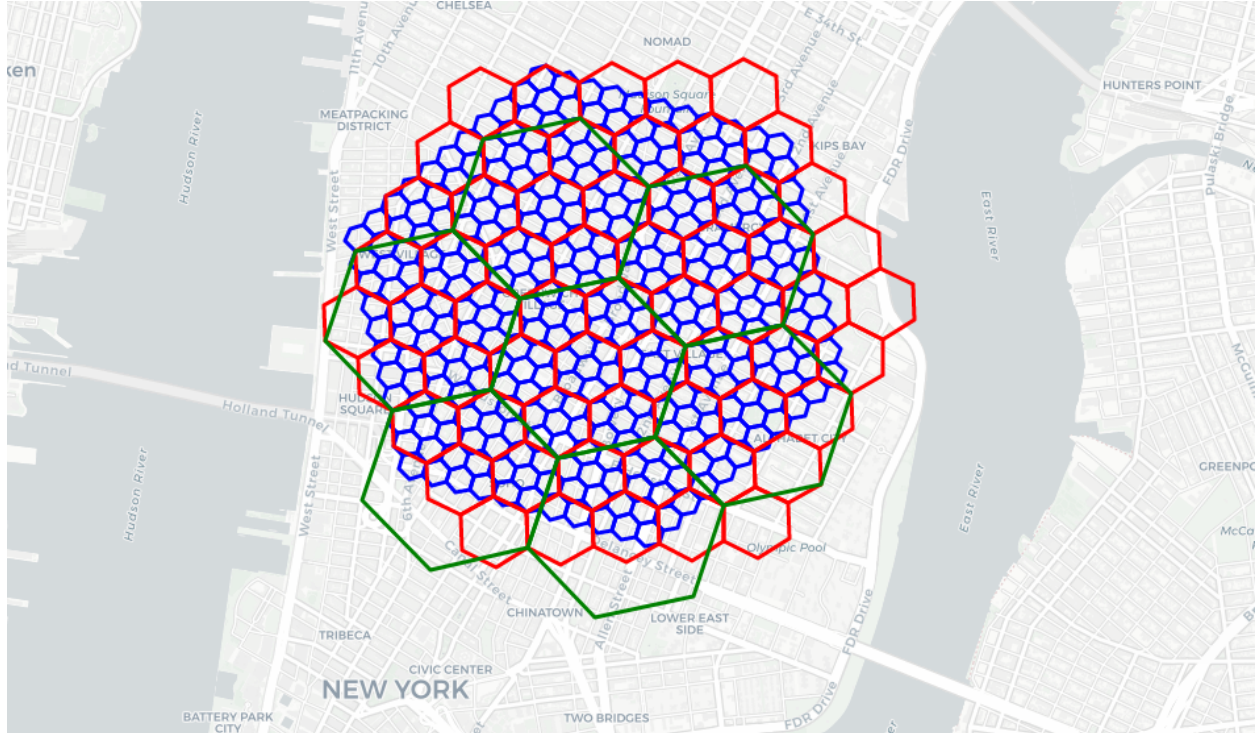


Figure 2: Illustration of the hexagons of the H3 index at different resolutions over Manhattan centred on the latitude/longitude coordinates 40.73129, -73.99288. Resolution 10 is shown in blue, resolution 9 in red and resolution 8 in green.

Initially, we considered representing each spatial point using a 768 dimensional vector learned through an autoencoder — a model renowned for its effectiveness in conventional contexts. However, we confronted a substantial challenge unique to the realm of geographical coordinates. Even the slightest deviations in these coordinates translated into significant errors in the real-world domain, as previously discussed in the introduction. This limitation prompted us to look for a more robust solution.

The H3 index offers a host of advantages ideally suited for our objectives. H3 represents geographical locations as hexagons as shown in figure 2, ensuring that any two neighbouring hexagons are always at an absolute distance of 1 unlike the S2 representation system [35]. The geometric nature of hexagons makes them less deformable at the poles. Furthermore, H3 provides multiple resolution levels, making it adaptable to various spatial scales. The 64-bit cell identifiers in H3 proved highly efficient for handling extensive geographical data, aligning seamlessly with the demands of big data applications. Unlike alternative methods [36], such as Geohash and Hexbin, H3 demonstrated reduced visual distortions when subjected to different map projections, ensuring the preservation of spatial fidelity.

In our research, we opted for a resolution level of 10, which effectively covers an area of approximately 1.5 hectares. To put it in perspective, this resolution corresponds to a square with sides of approximately 122 metres, roughly equivalent to the area of 1.4 football fields. This choice represents a balanced trade-off between the number of cells and computational efficiency, facilitating the practical implementation of our methodology. It’s important to note that pursuing greater precision in spatial representation could lead to diminishing returns, as GNSS inaccuracies could result in non-stop coordinate jumps, rendering excessively high resolutions impractical for our purposes.

To facilitate efficient representation and manipulation of H3 cells, we introduced the concept of a pseudo-octal representation. This involved discarding the initial 12 bits (Table 3 in A), considering a fixed resolution mode, and encoding the basic cell as a 2-character hexadecimal string. Each resolution level was then encoded in octal form, ensuring a consistent and concise representation that streamlined subsequent processing steps. Detailed algorithms for this transformation and its inverse can be found in algorithms 1 and 2.

Algorithm 1 Converts an H3 cell identifier to a pseudo-octal string representation.

Require: $cell$ ▷ a string representing the H3 cell identifier in hexadecimal format
Ensure: A pseudo-octal string representation of the given H3 cell identifier

```

 $i \leftarrow h3 :: str\_to\_int(cell)$ 
 $l \leftarrow []$ 
 $bc \leftarrow format(f \gg (52 - 7), 02x)$ 
for  $u$  from 42 down to 0 step  $-3$  do
     $digit \leftarrow ((f \gg u) \& 7) + ORD("0")$ 
    append  $char(digit)$  to  $l$ 
end for
return  $bc + join(l)$ 

```

▷ Example: $8a39690b4747fff \mapsto 1c55102643507777$

Algorithm 2 Converts a pseudo-octal cell identifier to a hexadecimal string representation.

Require: $cell$ ▷ a string representing the H3 cell identifier in pseudo-octal format
Ensure: A hexadecimal string representation of the given pseudo-octal cell identifier

```

 $bc \leftarrow cell[2]$ 
 $value \leftarrow (((1 \ll 7) | 10) \ll 7) | int(bc, 16)$ 
for each  $c \in cell[2:]$  do
     $value \leftarrow (value \ll 3) | int(c, 8)$ 
end for
return  $value$ 

```

▷ Example: $1c55102643507777 \mapsto 8a39690b4747fff$

Tokenisation played a pivotal role in managing our spatial representation. We considered each two-character basic cell as a single token and treated each resolution level as a distinct token. Since we chose resolution 10, all informative tokens after this resolution are non-relevant and were thus set to 7 (empty octal value, resolutions 11 to 15). We could have removed them or tokenised as a single token to reduce computational complexity at the cost of a more complex return to coordinates in longitude and latitude. However, we chose to maintain them in our methodology, and we discuss its implications for future refinements.

In the following sections, we look at the practical implementation of these choices, showing their impact on improving the prediction of maritime trajectories. Our meticulous approach to spatial representation and tokenisation prepares the ground for the transformative application of Causal Language Modelling (CLM) in maritime trajectory prediction, a promising way to raise the accuracy and efficiency of models in this domain.

4.2 Model Architecture: Mixtral8x7B

Our research leverages the powerful architecture provided by the Mixtral8x7B model [37]. This model is based upon the Mistral 7B architecture [38] and incorporates a Mixture of Experts approach [39, 40], significantly enhancing its capacity to handle complex tasks. The inclusion of a sliding window mechanism further sets it apart, allowing for an attention span of 2560 tokens—a feature particularly beneficial when dealing with lengthy trajectories. In our specific case, this translates to an attention span of over 2 hours, providing the ability to capture intricate patterns in maritime movements. Additionally, the utilisation of Grouped Query Attention not only facilitates faster inference but also reduces cache size requirements, ensuring efficient model operation.

The complete architecture configuration for our application is defined as follows in the table 1. This comprehensive architecture with 220M parameters is tailored to our maritime trajectory prediction task, offering the capacity and flexibility to handle the complexities of ship movement patterns.

Parameter	Value
Vocabulary Size	270
Hidden Size	1024
Sliding Window	256
Number of Hidden Layers	10
Number of Attention Heads	16
Number of Key-Value Heads	8
Number of Experts	8
Experts per Token	2

Table 1: Mixtral8x7B Model Configuration

4.3 Hardware, dataset and training process

The model was trained on a machine equipped with an Intel Core i9-13900K processor, an NVIDIA GeForce RTX 4090 graphics card with 24GB of RAM on a Manjaro 23.1.3 operating system. The model was implemented using the HuggingFace and the PyTorch frameworks. The training of the model took 175,000 steps using an Adam optimiser with an initial learning rate of 5 times 10^{-4} and a gradient accumulation of 8 (see B for the learning curves).

The dataset used to train the model comes from a capture we made ourselves and covers a period of one week in August 2023. The working area forms a rectangle with latitude/longitude coordinates $(-43.33, -88.59; 80.25, 168.34)$, but the majority of the trajectories are located in the North Sea, English Channel, Atlantic Ocean and Mediterranean Sea.

Tokenised trajectories exceeding the size of the model context are split into chunks of size 2560. We choose to keep the overlapping tokens and to set a padding with an attention mask to zero. It consists of 1,731,686 unique trajectories within a set of around 32 million H3 cells. After tokenisation, it consists of 4 billion tokens and, to date, we believe it is the largest set of trajectory data cleaned and prepared for trajectory forecasting. The entire captured dataset has been used for training and validation (respectively 85% and 15% of the dataset). The testing phase was carried out using another dataset that we captured on the fly during 3 days in February 2024 and represents approximately 15,000 cleaned trajectories.

4.4 Evaluation metric

To analyse the results, we propose utilising the Fréchet distance [41] given by the equation 1. The rationale behind this choice lies in its ability to capture the similarity between two trajectories while considering both spatial proximity and sequential order of points. The Fréchet distance, by comparing the geometric similarity between the actual and predicted trajectories, serves as a stringent measure of predictive fidelity. We implemented the algorithm using the Haversine function, a method commonly employed for calculating distances between points on the Earth’s surface due to its accuracy in spherical geometry.

Consider two curves A and B in the metric space S . The Fréchet distance between these curves is the infimum of the maximum distances between points on A and B , mapped through reparametrisations α and β of the interval $[0, 1]$. This distance measures the dissimilarity between A and B by evaluating the maximal spatial discrepancy across all possible point correspondences established by α and β . The metric d in S is the Haversine distance, as delineated in equation 2.

$$F(A, B) = \inf_{\alpha, \beta} \max_{t \in [0, 1]} \left\{ d \left(A(\alpha(t)), B(\beta(t)) \right) \right\}; \quad (1)$$

where d is the distance function of S defined in 2.

$$d: \begin{cases} L_1 = \frac{\varphi_2 - \varphi_1}{2} \\ L_2 = \frac{\lambda_2 - \lambda_1}{2} \\ \varphi_1, \varphi_2, \lambda_1, \lambda_2 \mapsto 2r \arcsin \left(\sqrt{\sin^2(L_1) + \cos(\varphi_1) \cos(\varphi_2) \sin^2(L_2)} \right) \\ [-90; 90] \times [-90; 90] \times [-180; 180] \times [-180; 180] \longrightarrow \mathbb{R}_+ \end{cases} \quad (2)$$

where r is the Earth’s radius, φ_1 and φ_2 are the latitudes, λ_1 and λ_2 are the longitudes.

4.5 Kalman filter

To the best of our knowledge, there is currently no method for predicting the trajectory of ships at any point on Earth and over a long distance without being adjusted to the actual observations that will be made during data capture. We have chosen to compare our method with Kalman filters [42]. Our model uses only GPS positions, specifically longitude (lon) and latitude (lat), to predict trajectories, and a prediction is represented by a matrix $G \in \mathbb{R}^{\tau \times 2}$ with τ the length of the prediction. In order to more closely align with our model, which utilises only the positions for predictions, we chose to include only four values in the state of the Kalman filter: the longitude (lon), the latitude (lat), and their velocities (v_{lon} and v_{lat}). Traditionally, Extended Kalman filters can include more complex data like sea current patterns. However, to reduce dependency to external data, we chose to reduce the number of parameters for our model and thus for the Kalman filter. The Kalman filter predicts a single state and must adapt to real observations in its update phase. However, real observations do not yet exist in our maritime case. We need to modify the Kalman filter to make it auto-regressive with a number of steps τ , considering that a predicted state becomes the truth. We have chosen to restrict ourselves to the prediction phase, as expressed in the following equation 3.

$$\begin{aligned}\hat{x}_{k|k-1} &= F_k x_{k-1} \\ P_{k|k-1} &= F_k P_{k-1} F_k^T + Q_k\end{aligned}\tag{3}$$

The state is a vector $x = (lat, lon, v_{lat}, v_{lon})$. The transition matrix $F_k \in \mathbb{R}^{4 \times 4}$ is as follows considering Δ_t the time between two points, in our case 60 seconds:

$$F_k = \begin{pmatrix} 1 & 0 & \Delta_t & 0 \\ 0 & 1 & 0 & \Delta_t \\ 0 & 0 & 1 & 0 \\ 0 & 0 & 0 & 1 \end{pmatrix}$$

We define Q_k to be the process noise covariance matrix as an identity matrix $\mathbb{R}^{4 \times 4}$ multiplied by a factor of 1×10^{-3} and $P_{k|k-1}$ to be the state covariance matrix as an identity matrix $\mathbb{R}^{4 \times 4}$.

5 Results and discussions

5.1 Metrics analysis

Our analysis of the predictive accuracy of ship trajectory models shown in the table 2, centred on the Fréchet distance as a key metric, reveals nuanced insights into the model’s performance in real-world navigation scenarios. By applying a stringent selection criterion, we isolated trajectories where the model’s predictions were not only completed but also exceeded a prediction length of η minutes, as observed in our prior analysis and where $\eta = med(\mathcal{X}) - 5$, with $med(\mathcal{X})$ the median of the series of prediction minutes \mathcal{X} . This filtration yielded a dataset conducive to a focused analysis on the effectiveness of our predictive model under conditions of substantial navigational complexity.

The violin plot in figure 3 shows a dense clustering of data points, meaning that the majority of the model’s predictions fall within lower Fréchet distance ranges. This indicates a high level of accuracy in predicting ship trajectories under a broad set of conditions. In practical terms, this suggests that the model is adept at capturing the essential patterns and dynamics of maritime movement in many scenarios, making it a reliable tool for planning and navigation in familiar waters or under standard operating conditions (see C and D).

The long tail extending into higher Fréchet distances highlights the limitations of the model in certain complex scenarios. These outliers represent instances where the predicted trajectory significantly deviates from the actual path taken by the ship. Such deviations could arise from unpredictable environmental factors (like sudden weather changes), complex maritime traffic conditions, or unique navigational challenges not fully encapsulated by the model’s parameters such as the trajectories of fishing boats, which are difficult to predict by taking only GNSS positions into account. These cases underscore the challenges of modelling the intricacies of real-world navigation, where unforeseen variables can impact a ship’s course.

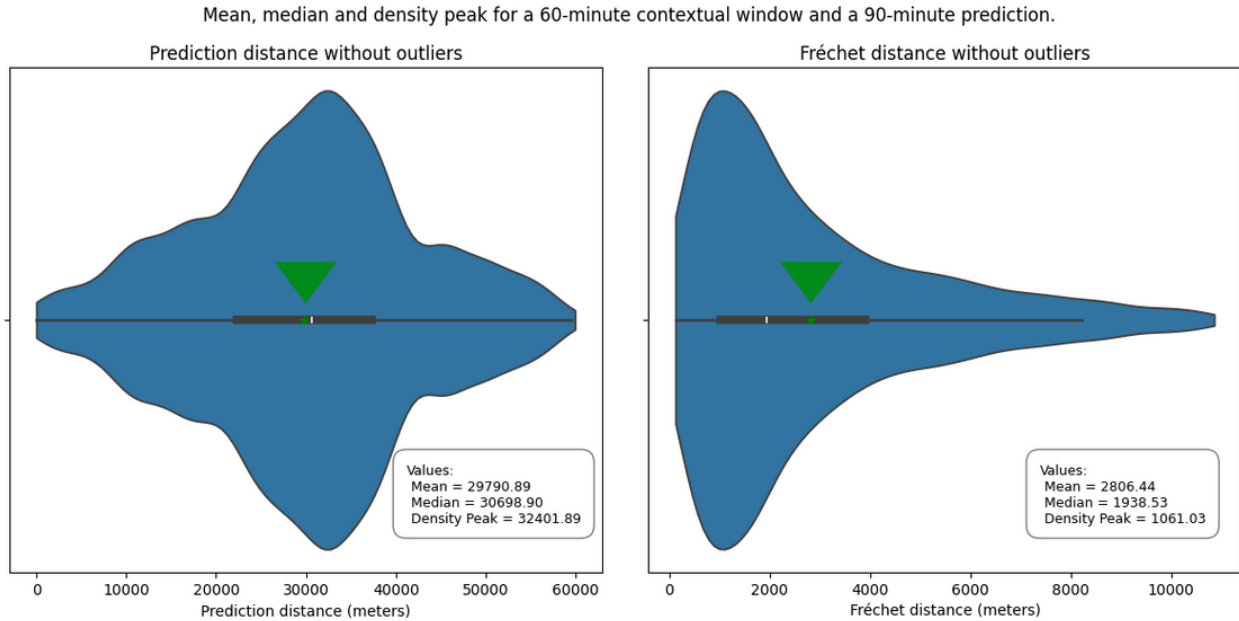


Figure 3: Violin plot of the prediction distance without outliers, highlighting the mean (green star, indicated by the green arrow head), median, and density peak for a context length of 60 minutes and a prediction length of 90 minutes. See figures 11, 12 and 13 in E for the full analysis.

The general effectiveness of the model in a wide range of conditions is a strong proof of its utility in maritime operations, offering a robust tool for route planning, risk assessment, and decision-making support. However, the instances of significant prediction error—reflected in the higher Fréchet distances—signal the need for caution. They suggest that reliance on the model should be balanced with situational awareness and potentially supplemented with real-time data and human expertise, especially in navigating complex or unfamiliar waters. By reducing instances of high Fréchet distances, we would improve the model’s reliability across a wider array of navigational scenarios.

Prediction	2560	5120 (x2)	7680 (x3)
Context			
Mean			
30 (540 tokens)	11.46%	18.30% (x1.60)	22.89% (x2.00)
60 (1080 tokens)	9.42%	18.84% (x2.00)	25.61% (x2.71)
100 (1800 tokens)	6.97%	14.78% (x2.12)	23.33% (x3.34)
Median			
30 (540 tokens)	7.80%	13.23% (x1.70)	17.54% (x2.24)
60 (1080 tokens)	6.31%	13.67% (x2.16)	19.46% (x3.08)
100 (1800 tokens)	4.88%	11.33% (x2.32)	17.82% (x3.65)
Density Peak			
30 (540 tokens)	4.51%	5.95% (x1.32)	10.33% (x2.29)
60 (1080 tokens)	3.27%	6.51% (x1.99)	7.98% (x2.44)
100 (1800 tokens)	2.67%	6.86% (x2.57)	8.55% (x3.20)

Table 2: Relative deviation between predictions and ground truth for mean, median and peak density. The context is expressed in minutes, while the prediction is expressed in the number of tokens generated. It can be seen that for a doubled distance, the relative error is approximately doubled, which suggests that the model has generalised sufficiently to produce a linear error.

The figure 4 highlights that the prediction error generally increases with the prediction distance, as shown by the comparison between (a) and (b). It is generally observed that the prediction errors are greater as the context length is reduced, and the prediction length is increased. On the other hand, we can see that, despite certain hallucinations

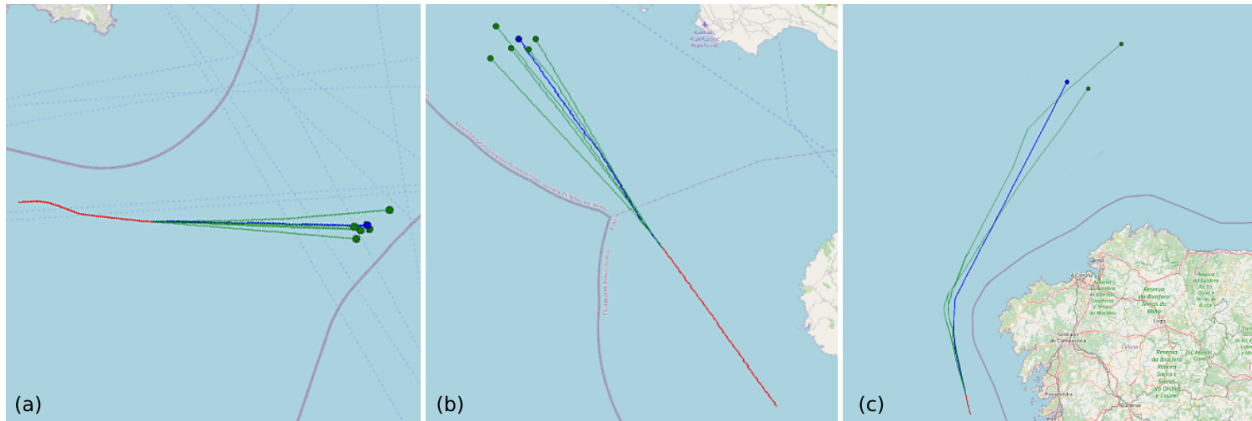


Figure 4: Path prediction performance comparison. This graph compares trajectory prediction performance for different configurations of context windows and prediction distances. (a) 60 minutes of context with a prediction at 90 minutes, (b) 100 minutes of context with a prediction at 90 minutes and (c) 60 minutes of context with a prediction at 20 hours. The colours represent the context window (red), the trajectories predicted by the model (green) and the actual trajectory (blue). We can see zigzags between the points due to the geometric arrangement of the hexagons. (a) and (b) are to the same scale, (c) is zoomed out.



Figure 5: Context (red), ground-truth (blue) and prediction (yellow) using a Kalman filter. The figure shows that the Kalman filters, in our use case, predict linear trajectories because they are auto-regressive, and they are not very sophisticated (e.g. no integration of headings and marine drift models). This seems to work very well when a ship is going straight along its route (a, b), but not so well when there are sharp bends or changes of direction (c).

which we will discuss later, the model seems to have generalised the nature of a trajectory, as shown in image (c) of figure 14 in F.

We compare our model to the Kalman filter on the same dataset. However, we did not apply the H3 transformation for the Kalman pass, as the filter is then less sensitive to trajectory zigzags. We changed the colour of the predictions to yellow for the Kalman filter in order to differentiate them from the green predictions of our model.

The figure 5 depicts the results of the Kalman filter. We notice that the Kalman filter appears to draw a straight vector from the last known position. As we know, our auto-regressive Kalman filter does not take into account the history of the ship and a Kalman filter is not designed to know the trends of other ships. We are trying to demonstrate here that the Kalman filter is not a totally reliable indicator for a ship because it has no knowledge of the ship's past, the ship's current trend or the shipping trend of other ships. However, we can qualify this by considering that a Kalman filter can be good and highly sufficient on a defined maritime route (for example for cargo ships and container ships) because these ships have straight trajectories.

5.2 Trajectory density

In our study, we aim to assess the veracity of ship trajectories by generating a set of thirty predictive paths. The primary objective is to evaluate the accuracy of these trajectories by examining the proximity of the centroid of a polygon, formed by the endpoints of the generated trajectories, to the actual ground truth position of the ship. This method provides an estimate of the reliability of the predictions made by our model.

We have observed two distinct scenarios in the outcomes of our analysis. In the first scenario depicted in figure 6, a significant majority of the trajectories coincide, indicating a high likelihood that these paths accurately reflect the ship's movement. This consensus among the trajectories suggests a precise and reliable prediction. In the second scenario, the generated trajectories vary widely, resulting in what could be described as chaos (figure 7, left). However, this dispersion does not necessarily indicate a flaw in the model but rather a multitude of possible paths the ship could take. In such cases, further analysis and additional context are required to ascertain the exact trajectory of the ship.

Lastly, it is crucial to highlight that some trajectories generated by our model are physically unfeasible for a ship to execute. We have coined the term "hallucinations" to describe these unachievable trajectories, a concept further elaborated in the following section of our paper. This distinction aids in refining the accuracy of our model by eliminating non-viable predictions and focusing on plausible trajectories.

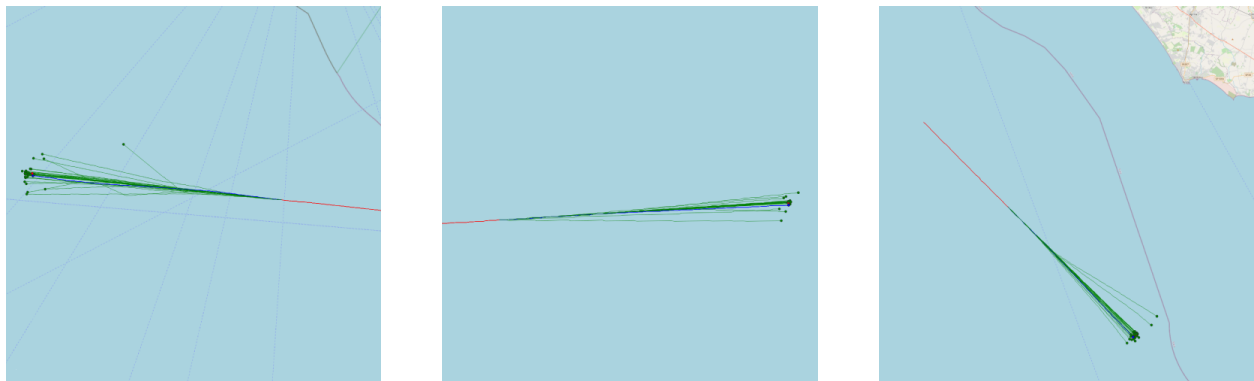


Figure 6: Illustration of the trajectory consensus phenomenon. This figure shows three examples of sets of trajectories where between 85 and 95% of the predicted trajectories align closely, representing a high degree of agreement between the model's predictions. Each set demonstrates the model's ability to accurately predict ship motion, highlighting the reliability of consensus trajectories in reflecting the actual navigation path.

5.3 Hallucination

In the development of this predictive model for ship trajectory forecasting, an interesting phenomenon that we called "hallucination" has been observed. This term is used to describe generated trajectories by the model that are not feasible for a ship to execute in reality. Examples of such unrealistic trajectories include abrupt U-turns, tight turns, and improbable GPS jumps, which are highly unlikely in our context. These anomalies can be visually identified in the model's output, as showcased in the subsequent figure 7.

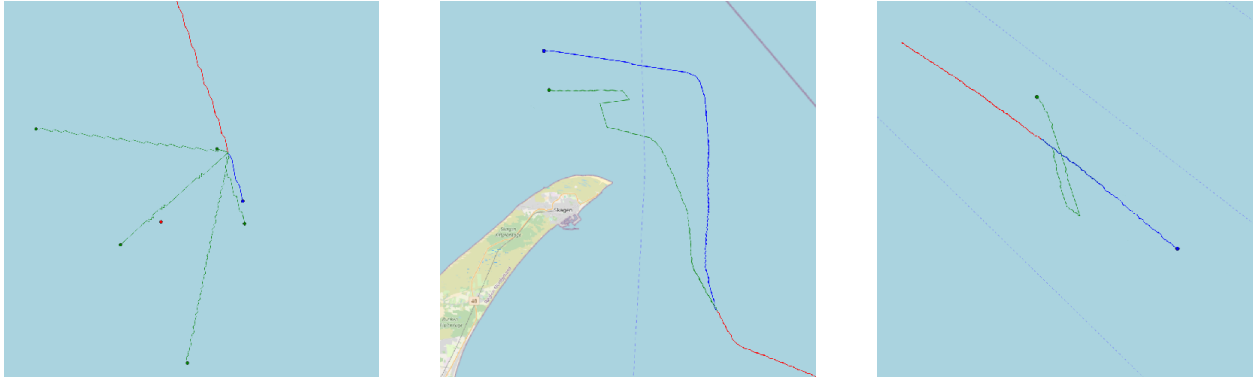


Figure 7: An example of the phenomena we have called "hallucinations". A red line represents the context used to generate the green trajectories. A blue line represents the ground truth. The red point is the barycentre of the polygon formed by the green points at the ends of the green trajectories.

Currently, there is no concrete explanation for the occurrence of these hallucinations. However, it is acknowledged that this phenomenon is exceedingly rare. Despite its infrequency, the ability to visually distinguish these erroneous outputs is crucial. Marine operation teams can easily identify these hallucinations, ensuring that such unrealistic predictions are not considered in practical navigation decisions.

To address and potentially mitigate the generation of hallucinatory trajectories, future research could explore the application of reinforcement learning solutions. By incorporating concepts of correct versus incorrect trajectories, techniques such as Reinforcement Learning from Human Feedback (RLHF) [43, 44, 45, 46, 47], Reinforcement Learning with Artificial Intelligence Feedback (RLAIF) [48], or Direct Preference Optimization (DPO) [49] might offer promising avenues for improvement. Additionally, integrating a positioning vector token within a pseudo-octal representation of the cell could enhance the spatial structure understanding of the model, promoting more realistic trajectory predictions.

This exploration into advanced learning methodologies and structural enhancements remains a prospective area of research. Such investigations could significantly refine the predictive accuracy and reliability of ship trajectory models, ensuring that hallucinations are effectively minimized or altogether eliminated in future iterations.

6 Conclusion

In conclusion, our foray into the H3 index system has significantly enhanced our approach to spatial data representation, particularly in the context of maritime trajectory prediction. The ability of the H3 index to reduce visual distortions across different map projections and to maintain spatial fidelity has been crucial in our work.

The introduction of a pseudo-octal representation for the H3 cells marked a pivotal point in our research. This innovative approach, involving the discarding of initial bits and encoding cells in a more compact format, significantly streamlined our data processing. The algorithms we developed for this transformation and its inverse showcase our commitment to enhancing the efficiency of spatial data manipulation.

Looking at the practical implementation of these choices, it becomes clear that they have impacted the prediction of maritime trajectories. Our methodical approach to spatial representation and tokenisation has laid the groundwork for the application of Causal Language Modelling (CLM) in this domain. The integration of CLM promises to improve maritime trajectory prediction, enhancing both the accuracy and efficiency of predictive models.

Although the Mixtral8x7B model architecture is very effective at capturing the complex patterns of maritime trajectories, we recognise the potential benefits of Fourier transforms. Recent advances, particularly in FNet [50], have demonstrated the usefulness of Fourier transforms in sequence modelling tasks. We believe that the application of Fourier transforms could further improve our model's ability to recognise additional patterns and nuances in ship trajectories, which could lead to even more accurate predictions. This line of exploration represents an intriguing future direction in our pursuit of improving the accuracy of maritime trajectory prediction.

This research not only contributes to the field of geospatial data analysis but also opens new pathways for future exploration, particularly in the application with advanced modelling techniques like CLM. We anticipate that our

findings and methodologies will pave the way for more sophisticated and accurate applications in maritime trajectory prediction and beyond.

Acknowledgement

I'd like to express my deepest gratitude to Jean-Daniel de Ambrogi, my Ph.D. colleague who has carefully reviewed my manuscript.

I am truly thankful for his insightful and constructive feedback, which has significantly improved the quality of my work. His time and attention are extremely valuable to me and I truly appreciate his dedication to my professional development.

References

- [1] Sepp Hochreiter and Jürgen Schmidhuber. Long short-term memory. *Neural computation*, 9(8):1735–1780, 1997.
- [2] Kyunghyun Cho, Bart Van Merriënboer, Caglar Gulcehre, Dzmitry Bahdanau, Fethi Bougares, Holger Schwenk, and Yoshua Bengio. Learning phrase representations using rnn encoder-decoder for statistical machine translation. *arXiv preprint arXiv:1406.1078*, 2014.
- [3] J.T. Connor, R.D. Martin, and L.E. Atlas. Recurrent neural networks and robust time series prediction. *IEEE Transactions on Neural Networks*, 5:240–254, 3 1994.
- [4] Mohammad Assaad, Romuald Boné, and Hubert Cardot. A new boosting algorithm for improved time-series forecasting with recurrent neural networks. *Information Fusion*, 9:41–55, 1 2008.
- [5] David Salinas, Valentin Flunkert, Jan Gasthaus, and Tim Januschowski. Deepar: Probabilistic forecasting with autoregressive recurrent networks. *International Journal of Forecasting*, 36:1181–1191, 7 2020.
- [6] Zulfiqar Khan, Tanveer Hussain, Amin Ullah, Seungmin Rho, Miyoung Lee, and Sung Baik. Towards efficient electricity forecasting in residential and commercial buildings: A novel hybrid cnn with a lstm-ae based framework. *Sensors*, 20:1399, 3 2020.
- [7] Ashish Vaswani, Noam Shazeer, Niki Parmar, Jakob Uszkoreit, Llion Jones, Aidan N Gomez, Łukasz Kaiser, and Illia Polosukhin. Attention is all you need. *Advances in neural information processing systems*, 30, 2017.
- [8] Tom Brown, Benjamin Mann, Nick Ryder, Melanie Subbiah, Jared D Kaplan, Prafulla Dhariwal, Arvind Neelakantan, Pranav Shyam, Girish Sastry, Amanda Askell, et al. Language models are few-shot learners. *Advances in neural information processing systems*, 33:1877–1901, 2020.
- [9] Alec Radford, Jeffrey Wu, Rewon Child, David Luan, Dario Amodei, Ilya Sutskever, et al. Language models are unsupervised multitask learners. *OpenAI blog*, 1(8):9, 2019.
- [10] Jacob Devlin, Ming-Wei Chang, Kenton Lee, and Kristina Toutanova. Bert: Pre-training of deep bidirectional transformers for language understanding. *arXiv preprint arXiv:1810.04805*, 2018.
- [11] Yuqi Nie, Nam H. Nguyen, Phanwadee Sinthong, and Jayant Kalagnanam. A time series is worth 64 words: Long-term forecasting with transformers. 11 2022.
- [12] Ailing Zeng, Muxi Chen, Lei Zhang, and Qiang Xu. Are transformers effective for time series forecasting? 5 2022.
- [13] Yong Liu, Tengge Hu, Haoran Zhang, Haixu Wu, Shiyu Wang, Lintao Ma, and Mingsheng Long. itransformer: Inverted transformers are effective for time series forecasting. 10 2023.
- [14] Haixu Wu, Tengge Hu, Yong Liu, Hang Zhou, Jianmin Wang, and Mingsheng Long. Timesnet: Temporal 2d-variation modeling for general time series analysis. 10 2022.
- [15] Haoyi Zhou, Shanghang Zhang, Jieqi Peng, Shuai Zhang, Jianxin Li, Hui Xiong, and Wancai Zhang. Informer: Beyond efficient transformer for long sequence time-series forecasting. In *Proceedings of the AAAI conference on artificial intelligence*, volume 35, pages 11106–11115, 2021.
- [16] Haixu Wu, Jiehui Xu, Jianmin Wang, and Mingsheng Long. Autoformer: Decomposition transformers with auto-correlation for long-term series forecasting. *Advances in Neural Information Processing Systems*, 34:22419–22430, 2021.
- [17] Uber. H3: Hexagonal hierarchical geospatial indexing system. <https://github.com/uber/h3>, 2018.

- [18] International Maritime Organization. *Revised guidelines for the onboard operational use of shipborne Automatic Identification Systems (AIS)*. IMO, December 2015. Adopted on 2 December 2015 (Agenda item 10).
- [19] Walter L. Sharp. *Geospatial Intelligence Support to Joint Operations*. DIANE Publishing Company, 2011.
- [20] Robert M. Clark. *Geospatial Intelligence. Origins and Evolution*. Georgetown University Press, 2020.
- [21] Yunyang Xiong, Zhanpeng Zeng, Rudrasis Chakraborty, Mingxing Tan, Glenn Fung, Yin Li, and Vikas Singh. Nystromformer: A nystrom-based algorithm for approximating self-attention. volume 35, pages 14138–14148, 2021.
- [22] Iz Beltagy, Matthew E Peters, and Arman Cohan. Longformer: The long-document transformer. *arXiv preprint arXiv:2004.05150*, 2020.
- [23] Rewon Child, Scott Gray, Alec Radford, and Ilya Sutskever. Generating long sequences with sparse transformers. *arXiv preprint arXiv:1904.10509*, 2019.
- [24] Ofir Press, Noah A Smith, and Mike Lewis. Train short, test long: Attention with linear biases enables input length extrapolation. *arXiv preprint arXiv:2108.12409*, 2021.
- [25] Zihang Dai, Zhilin Yang, Yiming Yang, Jaime Carbonell, Quoc V Le, and Ruslan Salakhutdinov. Transformer-xl: Attentive language models beyond a fixed-length context. *arXiv preprint arXiv:1901.02860*, 2019.
- [26] Jianlin Su, Murtadha Ahmed, Yu Lu, Shengfeng Pan, Wen Bo, and Yunfeng Liu. Roformer: Enhanced transformer with rotary position embedding. *Neurocomputing*, 568:127063, 2 2024.
- [27] Enmei Tu, Guanghao Zhang, Lily Rachmawati, Eshan Rajabally, and Guang Bin Huang. Exploiting ais data for intelligent maritime navigation: A comprehensive survey from data to methodology. *IEEE Transactions on Intelligent Transportation Systems*, 19:1559–1582, 5 2018.
- [28] Brian Murray and Lokukaluge Prasad Perera. A dual linear autoencoder approach for vessel trajectory prediction using historical ais data. *Ocean Engineering*, 209:107478, 8 2020.
- [29] Giuliana Pallotta, Michele Vespe, and Karna Bryan. Vessel pattern knowledge discovery from ais data: A framework for anomaly detection and route prediction. *Entropy*, 15:2218–2245, 2013.
- [30] Kexin Bao, Jinqiang Bi, Miao Gao, Yue Sun, Xuefeng Zhang, and Wenjia Zhang. An improved ship trajectory prediction based on ais data using mha-bigru. *Journal of Marine Science and Engineering*, 10, 6 2022.
- [31] BEAMer. *Rapport d’activités*. Feb 2022.
- [32] Xiang N Jiang Erico de Souza Ahmad Pesaranghader Baifan Hu, Daniel L Silver, Stan Matwin, Xiang Jiang, Erico N de Souza, Ahmad Pesaranghader, and Baifan Hu. Trajectorynet: An embedded gps trajectory representation for point-based classification using recurrent neural networks, 2017.
- [33] Duong Nguyen and Ronan Fablet. A transformer network with sparse augmented data representation and cross entropy loss for ais-based vessel trajectory prediction. *IEEE Access*, pages 1–1, 2024.
- [34] Duong Nguyen, Rodolphe Vadaine, Guillaume Hajduch, René Garello, and Ronan Fablet. A multi-task deep learning architecture for maritime surveillance using ais data streams. In *2018 IEEE 5th International Conference on Data Science and Advanced Analytics (DSAA)*, pages 331–340, 2018.
- [35] Google. S2 geometry: Computational geometry and spatial indexing on the sphere. <https://github.com/google/s2geometry>, 2015.
- [36] Kevin Sahr, Denis White, and A. Jon Kimerling. Geodesic discrete global grid systems. *Cartography and Geographic Information Science*, 30:121–134, 1 2003.
- [37] Albert Q. Jiang, Alexandre Sablayrolles, Antoine Roux, Arthur Mensch, Blanche Savary, Chris Bamford, Devendra Singh Chaplot, Diego de las Casas, Emma Bou Hanna, Florian Bressand, Gianna Lengyel, Guillaume Bour, Guillaume Lample, L lio Renard Lavaud, Lucile Saulnier, Marie-Anne Lachaux, Pierre Stock, Sandeep Subramanian, Sophia Yang, Szymon Antoniak, Teven Le Scao, Th ophile Gervet, Thibaut Lavril, Thomas Wang, Timoth e Lacroix, and William El Sayed. Mixtral of experts. 1 2024.
- [38] Albert Q. Jiang, Alexandre Sablayrolles, Arthur Mensch, Chris Bamford, Devendra Singh Chaplot, Diego de las Casas, Florian Bressand, Gianna Lengyel, Guillaume Lample, Lucile Saulnier, L lio Renard Lavaud, Marie-Anne Lachaux, Pierre Stock, Teven Le Scao, Thibaut Lavril, Thomas Wang, Timoth e Lacroix, and William El Sayed. Mistral 7b. 10 2023.
- [39] Noam Shazeer, Azalia Mirhoseini, Krzysztof Maziarz, Andy Davis, Quoc Le, Geoffrey Hinton, and Jeff Dean. Outrageously large neural networks: The sparsely-gated mixture-of-experts layer. 1 2017.
- [40] Barret Zoph, Irwan Bello, Sameer Kumar, Nan Du, Yanping Huang, Jeff Dean, Noam Shazeer, and William Fedus. St-moe: Designing stable and transferable sparse expert models. 2 2022.

- [41] M. Fréchet. *Sur la distance de deux lois de probabilité*. Feb 1957.
- [42] Rudolph Emil Kalman. A new approach to linear filtering and prediction problems. *Transactions of the ASME–Journal of Basic Engineering*, 82(Series D):35–45, 1960.
- [43] John Schulman, Sergey Levine, Philipp Moritz, Michael I. Jordan, and Pieter Abbeel. Trust region policy optimization. 2 2015.
- [44] John Schulman, Filip Wolski, Prafulla Dhariwal, Alec Radford, and Oleg Klimov. Proximal policy optimization algorithms. 7 2017.
- [45] James MacGlashan, Mark K Ho, Robert Loftin, Bei Peng, Guan Wang, David Roberts, Matthew E. Taylor, and Michael L. Littman. Interactive learning from policy-dependent human feedback. 1 2017.
- [46] Nisan Stiennon, Long Ouyang, Jeff Wu, Daniel M. Ziegler, Ryan Lowe, Chelsea Voss, Alec Radford, Dario Amodei, and Paul Christiano. Learning to summarize from human feedback. 9 2020.
- [47] Long Ouyang, Jeff Wu, Xu Jiang, Diogo Almeida, Carroll L. Wainwright, Pamela Mishkin, Chong Zhang, Sandhini Agarwal, Katarina Slama, Alex Ray, John Schulman, Jacob Hilton, Fraser Kelton, Luke Miller, Maddie Simens, Amanda Askell, Peter Welinder, Paul Christiano, Jan Leike, and Ryan Lowe. Training language models to follow instructions with human feedback. 3 2022.
- [48] Harrison Lee, Samrat Phatale, Hassan Mansoor, Thomas Mesnard, Johan Ferret, Kellie Lu, Colton Bishop, Ethan Hall, Victor Carbune, Abhinav Rastogi, and Sushant Prakash. RLaiF: Scaling reinforcement learning from human feedback with ai feedback. 9 2023.
- [49] Rafael Rafailov, Archit Sharma, Eric Mitchell, Stefano Ermon, Christopher D. Manning, and Chelsea Finn. Direct preference optimization: Your language model is secretly a reward model. 5 2023.
- [50] James Lee-Thorp, Joshua Ainslie, Ilya Eckstein, and Santiago Ontanon. Fnet: Mixing tokens with fourier transforms. *arXiv preprint arXiv:2105.03824*, 2021.

A H3 Index Bit Layout

Start	Bits	Type
0	1	Reserved
1	4	Index Mode
5	3	Mode-Dependent
8	4	Resolution
12	7	Base Cell
19	3	Res 1 digit
22	3	Res 2 digit
25	3	Res 3 digit
28	3	Res 4 digit
31	3	Res 5 digit
34	3	Res 6 digit
37	3	Res 7 digit
40	3	Res 8 digit
43	3	Res 9 digit
46	3	Res 10 digit
49	3	Res 11 digit
52	3	Res 12 digit
55	3	Res 13 digit
58	3	Res 14 digit
61	3	Res 15 digit

Table 3: H3 Index Bit Layout

B Learning curves

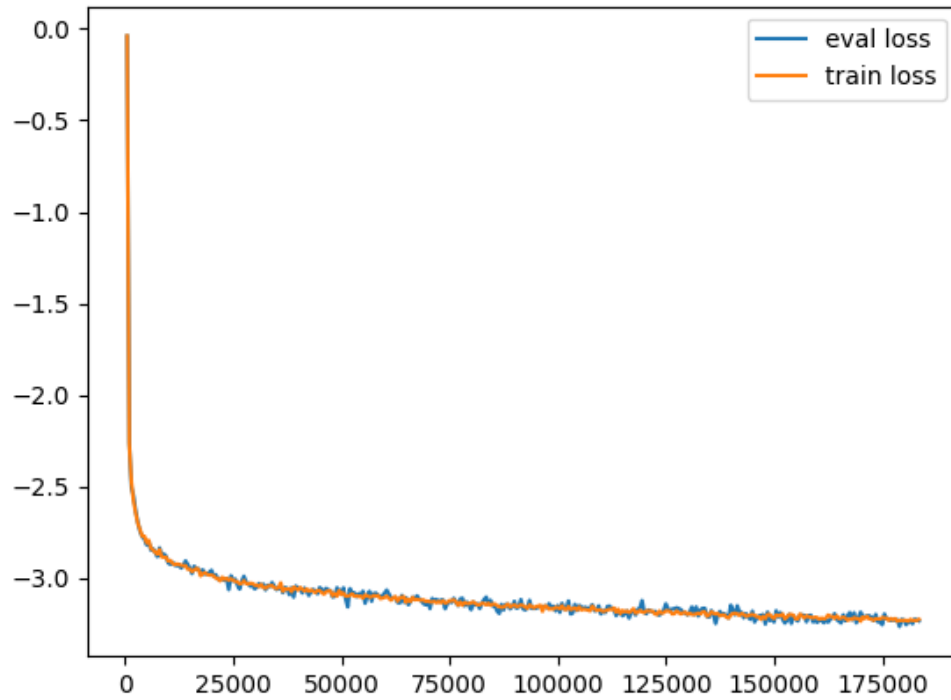


Figure 8: Unified training and evaluation loss curves. It shows the loss value compared to the number of steps in the training process. Convergence of training (orange) and evaluation (blue) loss curves indicates effective model generalisation without overfitting.

C Density plot of Fréchet distance versus prediction distance

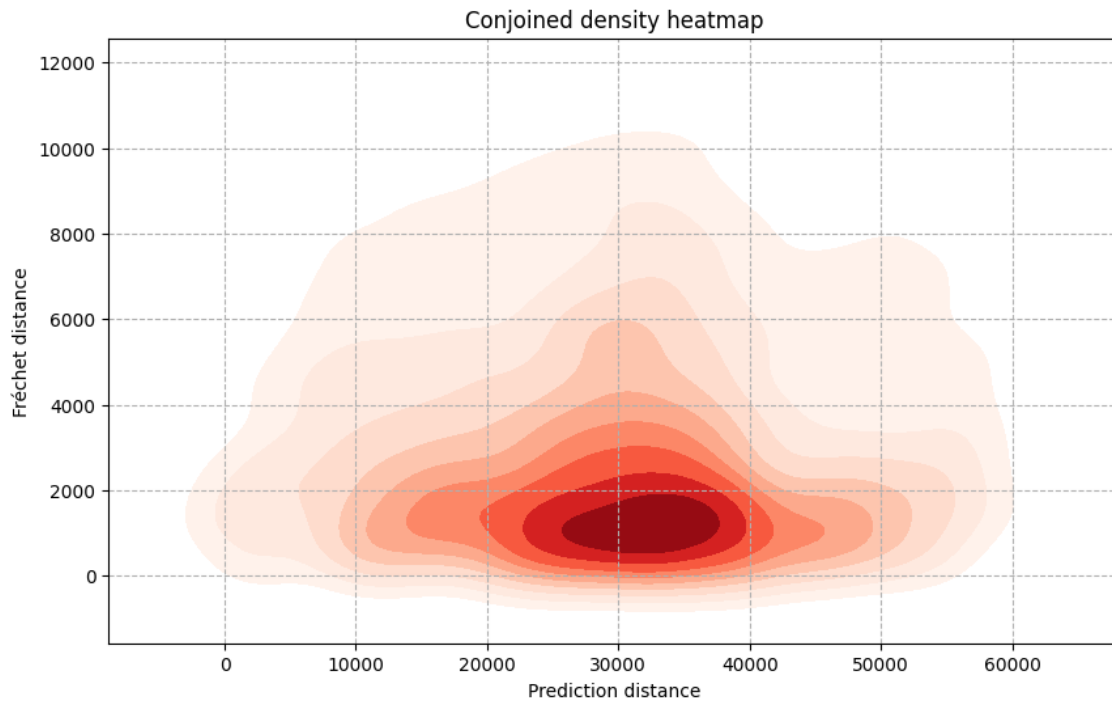


Figure 9: Graph showing the density of the Fréchet distance in metres compared with the prediction distance in metres for 90-minute predictions with 60 minutes of context. We can see that the errors measured by the Fréchet distance are minimal for prediction lengths of around 30km. Prediction distances that are too short or too long can be interpreted as teleportations or hallucinations.

D Example of a river prediction

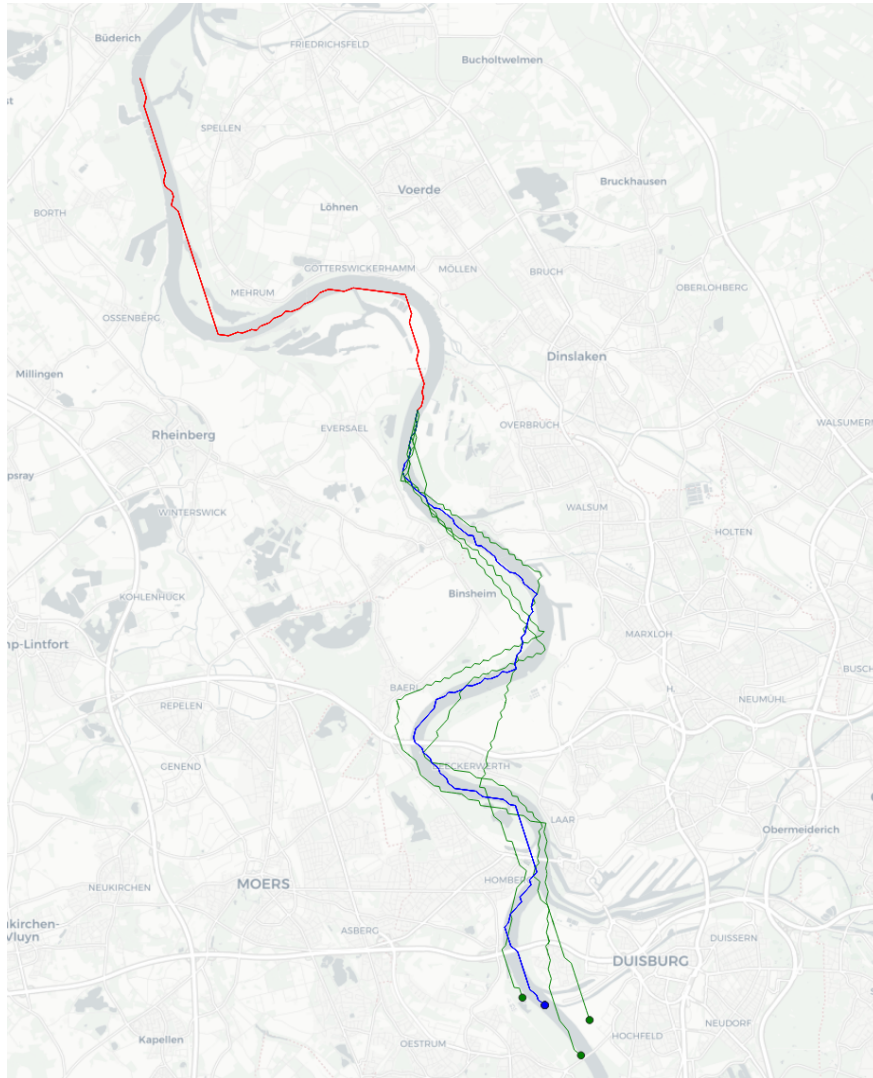


Figure 10: Illustration of a prediction of a ship's trajectory in a river. The context is represented by a 60 minutes long red line, the 155 minutes long green lines represent predictions. The ground truth is shown in blue. It is interesting to note that accuracy in these areas is lower, notably due to the inaccuracy of GNSS.

E Distribution of predictions

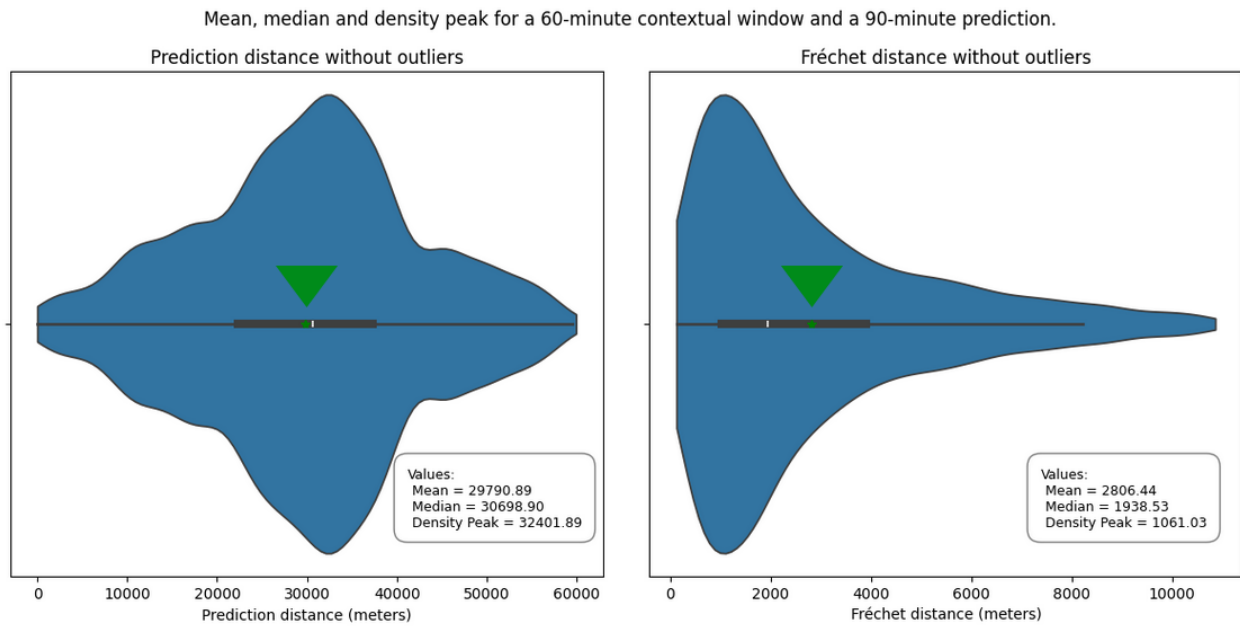


Figure 11: Violin plot of the prediction distance without outliers, highlighting the mean (green star), median, and density peak for a context length of 60 minutes and a prediction length of 90 minutes.

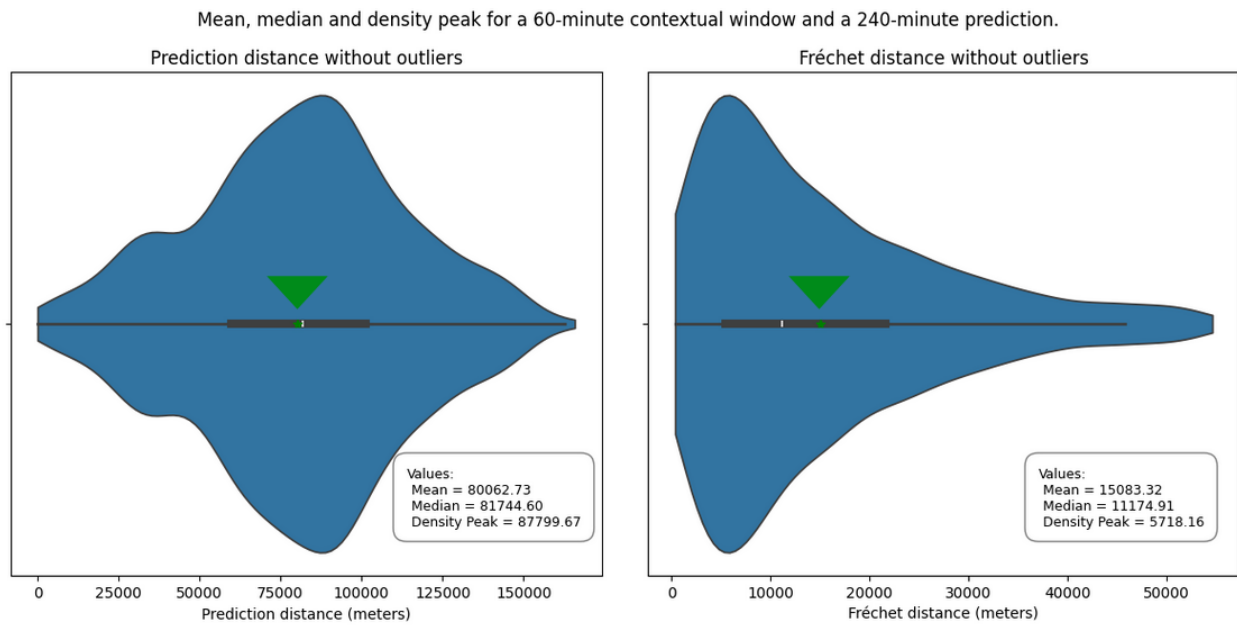


Figure 12: Violin plot of the prediction distance without outliers, highlighting the mean (green star), median, and density peak for a context length of 60 minutes and a prediction length of 240 minutes.

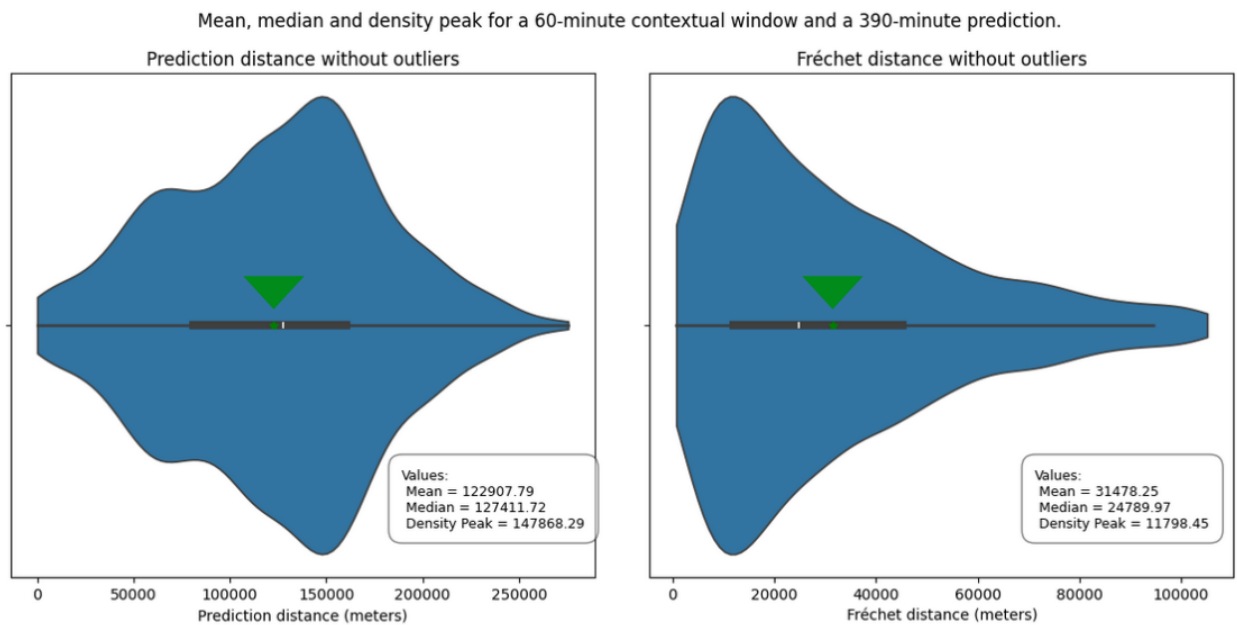


Figure 13: Violin plot of the prediction distance without outliers, highlighting the mean (green star), median, and density peak for a context length of 60 minutes and a prediction length of 390 minutes.

F Multiple trajectories grid

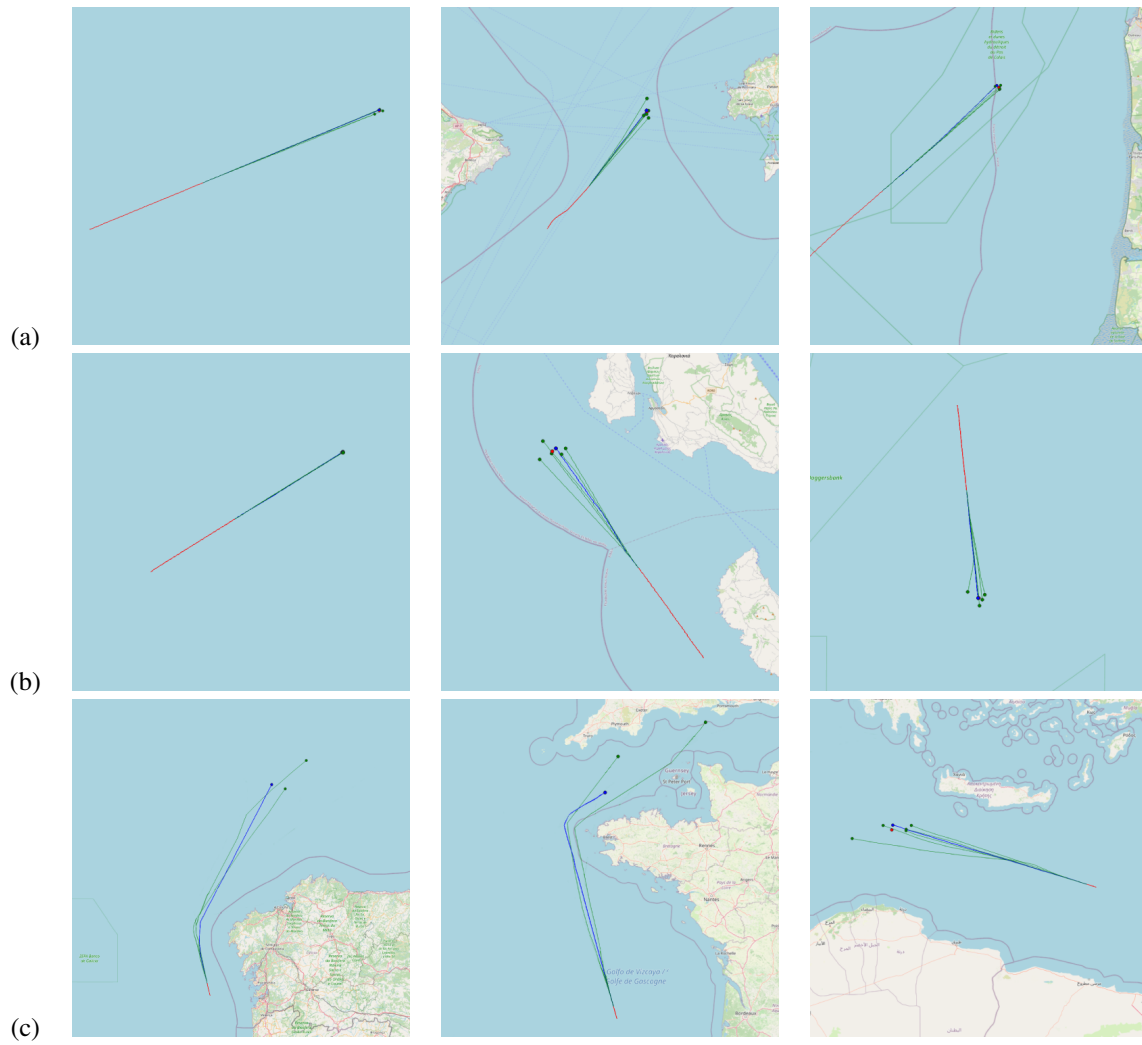


Figure 14: Zoom out path prediction performance comparison of figure 4.